Single-Molecule Detection in Liquids by Laser-Induced Fluorescence

PETER M. GOODWIN,* W. PATRICK AMBROSE, AND RICHARD A. KELLER

Chemical Science and Technology Division, Los Alamos National Laboratory, Los Alamos, New Mexico 87545

Received July 1, 1996

Introduction

Laser-induced fluorescence (LIF) detection of single fluorescent molecules represents the ultimate level of sensitivity for fluorescence-based chemical assays. This has been demonstrated by a number of groups for a variety of fluorescent molecules dissolved in liquids under ambient conditions. The rapidly growing research effort in the field of single-molecule detection (SMD) in liquids is reviewed by Keller[1] and Barnes.[2] Fluorescence detection sensitivity in liquids has improved significantly, especially in flow, during the past two decades. Figure 1 shows the state of the art in terms of the minimum number of detectable fluorochromes as a function of time during this period. Circles are results obtained for analyte dissolved in flowing sample streams, boxes represent results obtained with fluorescence microscopy of static samples, diamonds represent fluorescence correlation spectroscopy measurements on static (diffusing) samples, and triangles represent detection of analyte dissolved in levitated microdroplets. By the early 1990s, detection of single rhodamine 6G fluorochromes was demonstrated in flow.[3,4] Subsequent work demonstrated the spectral identification of single fluorochromes[5] as well as the measurement of single-molecule fluorescence lifetimes.[5,6]

Fluorescence detection has long been used to study and characterize chemical and biochemical systems. Improvements in detection sensitivity have allowed these studies to be extended down to the single-molecule level. We are developing flow-based SMD methods to sequence and measure the length (size) of single DNA fragments.[7] Single DNA fragment sequencing offers the potential for read lengths in the range of 10^4 base pairs (bp); electrophoresis-based methods have read lengths approaching 10^3 bp. Flow-based, single fragment DNA sizing has been demonstrated for both linear and supercoiled P1 artificial chromosomes up to 167 kilobase pairs in length and is expected to be useful for rapid, accurate characterization of clone libraries.[8] Pulsed field gel electrophoresis methods, currently used to size such large fragments, require tens of hours for separation versus minutes for single DNA fragment sizing. Single-molecule sensitivity has been achieved in conventional capillary electrophoresis separations of DNA[9] and fluorescent proteins.[10] Other work has demonstrated separation of single DNA fragments and fluorescent protein molecules by measurement of single-molecule electrophoretic drift times between two picoliter probe volumes separated by a fraction of a millimeter.[11] Fluorescence detection has been used to measure reactivities of individual lactate dehydrogenase molecules based upon a single enzyme molecule's ability to catalyze repetitively a weakly fluorescent substrate to a highly fluorescent product that is subsequently detected and quantified.[12] Another group has measured reactivities and activation energies of individual alkaline phosphatase enzyme molecules and determined that this enzyme is catastrophically denatured; that is, the activity of an individual enzyme molecule does not gradually decrease but falls abruptly.[13] Other work has resulted in the visualization of individual adenosine triphosphate (ATP) hydrolysis reactions on single myosin molecules using low background epifluorescence microscopy of single fluorescently labeled myosin and ATP molecules.[14] Single-molecule fluorescence detection techniques have been

Peter M. Goodwin received his B.S. degree in physics from the California Institute of Technology in 1980 and a Ph.D. in applied and engineering physics from Cornell University in 1989. He held postdoctoral positions at the IBM Technology Laboratory, Endicott, NY, and at Los Alamos National Laboratory, Los Alamos, NM. He is currently a staff member in the Chemical Science and Technology Division at Los Alamos. His research interests are in the areas of laser spectroscopy and ultrasensitive detection.

W. Patrick Ambrose received his B.S. in physics (magna cum laude) from California State University, Northridge, in 1982. Pat received his M.S. (1986) and Ph.D. (1989) in solid state physics from Cornell University; Prof. A. J. Sievers was his thesis advisor. Pat held a "Visiting Scientist" position (Postdoctoral Fellowship) at IBM's Almaden Research Center from 1989 to 1991; Dr. W. E. Moerner was Pat's postdoctoral supervisor at IBM. From 1991 to 1993 Pat held a Director's Funded Postdoctoral Fellowship at Los Alamos National Laboratory; Dr. Richard A. Keller was Pat's postdoctoral supervisor at Los Alamos. Since 1993, Pat has been a staff member at Los Alamos. Pat's main interests involve challenging research in sensitive optical detection, including fundamental studies of single fluorescent molecules.

Richard A. Keller received his B.S. degree from Allegheny College in 1956 and his Ph.D. from the University of California, Berkeley, in 1961. Keller was on the faculty at the University of Oregon from 1960 to 1963 and at the National Bureau of Standards, Washington, DC, from 1963 to 1976. Keller joined Los Alamos National Laboratory in 1976. He is currently a Laboratory Fellow in the Chemical Science and Technology Division at Los Alamos. Keller's research interests are in the development and characterization of new laser-based analytical techniques. In particular, he is interested in the application of single-molecule detection to analytical measurements.

* To whom correspondence should be addressed.

(1) Keller, R. A.; Ambrose, W. P.; Goodwin, P. M.; Jett, J. H.; Martin, J. C.; Wu, M. *Appl. Spectrosc.* **1996**, *50*, A12−A32.
(2) Barnes, M. D.; Whitten, W. B.; Ramsey, J. M. *Anal. Chem.* **1995**, *67*, A418−A423.
(3) Shera, E. B.; Seitzinger, N. K.; Davis, L. M.; Keller, R. A.; Soper, S. A. *Chem. Phys. Lett.* **1990**, *174*, 553−557.
(4) Soper, S. A.; Shera, E. B.; Martin, J. C.; Jett, J. H.; Hahn, J. H.; Nutter, H. L.; Keller, R. A. *Anal. Chem.* **1991**, *63*, 432−437.
(5) Soper, S. A.; Davis, L. M.; Shera, E. B. *J. Opt. Soc. Am. B* **1992**, *9*, 1761−1769.
(6) Wilkerson, C. W., Jr.; Goodwin, P. M.; Ambrose, W. P.; Martin, J. C.; Keller, R. A. *Appl. Phys. Lett.* **1993**, *62*, 2030−2032.
(7) Ambrose, W. P.; Goodwin, P. M.; Jett, J. H.; Johnson, M. E.; Martin, J. C.; Marrone, B. L.; Schecker, J. A.; Wilkerson, C. W., Jr.; Keller, R. A.; Haces, A.; Shih, P. J.; Harding, J. D. *Ber. Bunsen-Ges. Phys. Chem.* **1993**, *97*, 1535−1542.
(8) Huang, Z.; Petty, J. T.; O'Quinn, B.; Longmire, J. L.; Brown, N. C.; Jett, J. H.; Keller, R. A. *Nucleic Acids Res.*, in press.
(9) Haab, B. B.; Mathies, R. A. *Anal. Chem.* **1995**, *67*, 3253−3260.
(10) Chen, D. Y.; Dovichi, N. J. *Anal. Chem.* **1996**, *68*, 690−696.
(11) Castro, A.; Shera, E. B. *Anal. Chem.* **1995**, *67*, 3181−3186.
(12) Xue, Q.; Yeung, E. S. *Nature* **1995**, *373*, 681−683.
(13) Craig, D. B.; Arriaga, E. A.; Wong, J. C. Y.; Dovichi, N. J. *J. Am. Chem. Soc.* **1996**, *118*, 5245−5253.
(14) Funatsu, T.; Harada, Y.; Tokunaga, M.; Saito, K.; Yanagida, T. *Nature* **1995**, *374*, 555−559.

S0001-4842(95)00250-0 CCC: $12.00

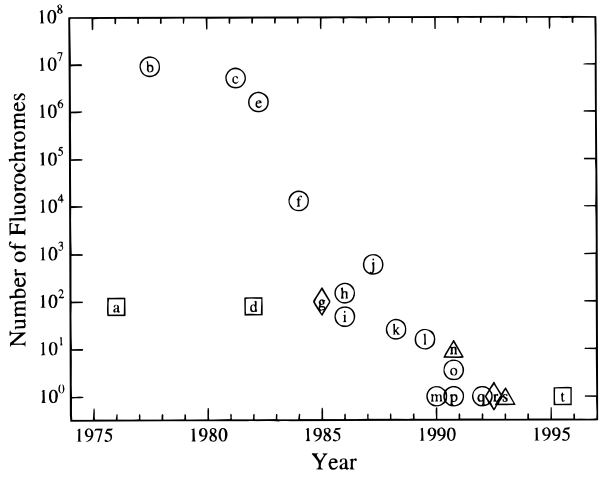

Figure 1. Improvement in the state of the art of ultrasensitive fluorescence detection in liquids. Detection limits in terms of the minimum number of detectable fluorochromes for various techniques are plotted. Circles represent measurements made in flow, triangles represent measurements on levitated microdroplets, boxes represent fluorescence microscopy of static samples, and diamonds represent fluorescence correlation spectroscopy measurements on static (diffusing) samples. References for each point on the graph are as follows: (a) Hirschfeld, T. *Appl. Opt.* **1976**, *15*, 2965−2966. (b) Diebold, G. J.; Zare, R. N. *Science* **1977**, *196*, 1439−1441. (c) Kelly, T. A.; Christian, G. D. *Anal. Chem.* **1981** , *53*, 2110−2114. (d) Barak, L. S.; Webb, W. W. *J. Cell Biol.* **1981**, *90*, 595−604. (e) Folestad, S.; Johnson, L.; Josefsson, B.; Galle, B. *Anal. Chem.* **1982**, *54*, 925−929. (f) Dovichi, N. J.; Martin, J. C.; Jett, J. H.; Trkula, M.; Keller, R. A. *Anal. Chem.* **1984**, *56* , 348−354. (g) Kask, P.; Piksarv, P.; Mets, Ü. *Eur. Biophys.* **1985**, *12*, 163−166. (h) Watson, J. V.; Walport, M. J. *J. Immunol. Methods* **1986**, *39*, 171−175. (i) Mathies, R. A.; Stryer, L. Single-Molecule Fluorescence Detection. In *Applications of Fluorescence in the Biomedical Sciences*, Taylor, D. L., Waggoner, A. S., Lanni, F., Murphy, R. F., Birge, R. R., Eds.; Alan R. Liss, Inc.: New York, 1986. (j) Nguyen, D. C.; Keller, R. A.; Trkula, M. *J. Opt. Soc. Am. B* **1987**, *4*, 138−143. (k) Nguyen, D. C.; Keller, R. A.; Jett, J. H.; Martin, J. C. *Anal. Chem.* **1987**, *59*, 2158−2161. (l) Peck, K.; Stryer, L.; Glazer, A. N.; Mathies, R. A. *Proc. Natl. Acad. Sci. U.S.A.* **1989**, *86*, 4087−4091. (m) Shera, E. B.; Seitzinger, N. K.; Davis, L. M.; Keller, R. A.; Soper, S. A. *Chem. Phys. Lett.* **1990**, *174*, 553−557. (n) Ramsey, J. M.; Whitten, W. B. *Anal. Chem.* **1991**, *63*, 1027−1031. (o) Hahn, J. H.; Soper, S. A.; Nutter, H. N.; Martin, J. C.; Jett, J. H.; Keller, R. A. *Appl. Spectrosc.* **1991**, *45*, 743−746. (p) Soper, S. A.; Hahn, J. H.; Nutter, H. L.; Martin, J. C.; Jett J. H.; Keller, R. A. *Anal. Chem.* **1991**, *63* , 432−437. (q) Soper, S. A.; Davis, L. M.; Shera, E. B. *J. Opt. Soc. Am. B* **1992**, *139*, 1761−1769. (r) Rigler, R.; Mets, Ü. *Proc. SPIE* **1992**, *1921*, 239−248. (s) Barnes, M. D.; Ng, K. C.; Whitten, W. B.; Ramsey, J. M. *Anal. Chem.* **1993**, *65*, 2360−2365. (t) Funatsu, T.; Harada, Y.; Tokunaga, M.; Saito, K.; Yanagida, T. *Nature* **1995**, *374*, 555−559. Schmidt, Th.; Schütz, G. J.; Baumgartner, W.; Gruber, H. J.; Schindler, H. *J. Phys. Chem.* **1995**, *99*, 17662−17668.

used to study intramolecular conformational transitions,[15] directly observe singlet−triplet intersystem crossings,[16,17] and study the photochemistry[18] of single molecules in solution. Experiments such as these eliminate the ensemble averaging that is often the result of measurements on bulk samples and allow the direct measurement of molecular property distributions. In this Account we describe SMD techniques developed at Los Alamos National Laboratory and

(15) Edman, L.; Mets, Ü.; Rigler, R. *Exp. Tech. Phys.* **1995**, *41*, 157−163.
(16) Nie, S.; Chiu, D. T.; Zare, R. N. *Science* **1994**, *266*, 1018−1021.
(17) Nie, S.; Chiu, D. T.; Zare, R. N. *Anal. Chem.* **1995**, *67*, 2849−2857.
(18) Wu, M.; Goodwin, P. M.; Ambrose, W. P.; Keller, R. A. *J. Phys. Chem.*, in press.

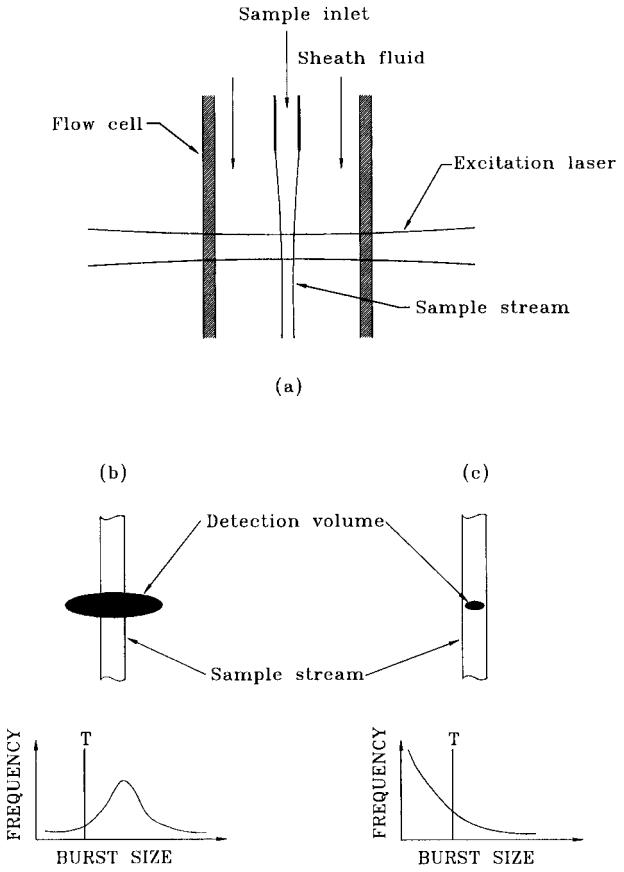

Figure 2. Delivery of sample to a detection volume. (a) Schematic of a sheath flow cuvette showing a hydrodynamically focused sample stream intersecting the excitation laser beam. (b) A small sample stream passing through a large probe volume. Below, size distribution of photon bursts detected from analyte molecules in the sample stream. A threshold for burst detection is shown with the vertical line labeled T. The majority of molecules in the sample stream are detected. (c) A large sample stream crossing a small probe volume. Below, size distribution of photon bursts detected from analyte molecules in the sample stream. Many of the molecules miss the probe volume entirely or give photon bursts below the detection threshold, T.

discuss their application to flow-based, single DNA fragment sequencing and sizing.

Single-Molecule Detection

Approach. The design of our fluorescence detection apparatus is based on that of a flow cytometer. As shown in Figure 2a, sample is introduced into a sheath flow upstream of a detection volume. Hydrodynamic focusing[19] by the sheath flow forms the sample into a narrow stream that intersects the detection volume. This arrangement allows the sample to be probed far away from the flow chamber walls, which are a major source of scattered excitation light and fluorescence background. The basis of SMD in flowing sample streams is excitation of a fluorescent molecule, as it flows through an excitation laser beam, at a rate sufficient to cause it to emit a burst of photons large enough to be detectable above background scatter and fluorescence. Because of solvent−molecule interactions, a solvated fluorescent molecule can be treated

(19) Kachel, V.; Fellner-Feldegg, H.; Menke, E. Hydrodynamic Properties of Flow Cytometry Instruments. In *Flow Cytometry and Sorting*, 2nd ed.; Melamed, M. R., Lindmo, T., Mendelsohn, M. L., Eds.; J. Wiley & Sons, Inc.: New York, 1990.

as a three-level system consisting of singlet ground ($S0$) and first excited ($S1$) state manifolds and an intermediate energy triplet state manifold ($T1$). A laser, tuned near the $S0 \rightarrow S1$ absorption maximum, excites transitions from $S0$ to high-lying rovibrational levels of $S1$ which undergo rapid (<1 ps) nonradiative decay to low-lying $S1$ levels. Fluorescence emission originates from radiative transitions (τ_f typically less than 10 ns) from these levels to high-lying rovibrational levels of $S0$. Optical saturation (ground state depletion) limits the maximum rate that a molecule can be cycled between $S0$ and $S1$ to $(\tau_f)^{-1} \approx 10^8$ s^{-1}. Population of the relatively long-lived triplet state ($\tau_p \approx 10^{-6} - 10^{-3}$ s) through spin-forbidden $S1 \rightarrow T1$ transitions temporarily halts fluorescence emission from the molecule. Such "triplet shelving" lowers the saturated fluorescence emission rate. Photophysical constants that determine the suitability of a fluorescent molecule for SMD are the (1) absorption cross-section, σ, (2) fluorescence quantum yield, Φ_f, the fraction of excitations to $S1$ that result in fluorescence emission, and (3) photodestruction quantum yield, Φ_d, the fraction of excitations to $S1$ that result in irreversible photochemical alteration of the molecule. The average number photons emitted by a molecule prior to photodestruction is Φ_f / Φ_d. Fluorochromes typically used for SMD have $\sigma \approx 10^{-16}$ cm^2, $\Phi_f > 0.1$, and $\Phi_d \lesssim 10^{-5}$, resulting in the emission of $\sim 10^5$ photons before photodestruction.

The challenge of SMD in liquids is the detection of fluorescence bursts from single molecules in the presence of a background due to scattered light and fluorescence from the solvent and any dissolved impurities in the detection volume (the illuminated region in the detector's field of view). For example, under ambient conditions, a region enclosing a $10 \times 10 \times 10$ μm^3 (10^{-12} L = 1 pL) volume contains approximately 3×10^{13} water molecules. Despite the small Raman scattering cross-section of a single water molecule ($\sim 10^{-28}$ cm^2 at 488 nm[20]), the large number of molecules in this volume contribute to a total Raman scattering area that is larger than the absorption cross-section of a typical fluorochrome ($\sim 10^{-16}$ cm^2). Even with spectral band-pass filters, residual Raman and Rayleigh scattered light can comprise the majority of the background.

For a 1 pL detection volume, a fluorescent impurity present at a concentration of 1.7×10^{-12} M will give an average of one impurity molecule in the detection volume at any time. If the impurity is strongly fluorescent within the detection spectral band-pass, then it will give a large, "bursting" background that will overwhelm photon bursts due to analyte molecules. If the impurity is only weakly fluorescent, it will contribute a quasi-continuous, "nonbursting" background.

A simple way to reduce background is to minimize the detection volume. Probe volumes as small as 0.2 fL (10^{-15} L = 1 μm^3 = 1 fL) have been obtained using laser confocal-microscopy techniques. With such small volumes, fluorescence bursts from single fluorochromes can be detected easily.[16,17,21] A drawback of using extremely small volumes is the difficultly of producing sufficiently small sample streams to ensure that analyte molecules are delivered through the center of the probe volume for efficient detection. This is illustrated schematically in panels b and c of Figure 2. The size and shape of the detection volume are determined by the spatially dependent product of the excitation intensity, $I(\vec{r})$, and optical collection efficiency, $\eta(\vec{r})$, where $\vec{r}$ is the position in the object volume.[22,23] In the absence of photobleaching, a fluorescent molecule crossing the probe volume will cause a path ($\vec{r}(t)$) dependent burst of photons, proportional to $\int (I(\vec{r}(t))\, \eta(\vec{r}(t)))\, dt$ in size, to be imaged on the detector. Molecules passing near the edges of the detection volume will give smaller bursts than those crossing the center where $I(\vec{r})\, \eta(\vec{r})$ is peaked. The relative sizes of the sample stream and detection volume determine the shape of the size distribution of detected bursts. For a sufficiently small sample stream, all of the analyte molecules pass near the center of the probe volume and the burst size distribution is peaked away from zero as shown in Figure 2b. If the sample stream is too large, some molecules cross near the edges of the probe volume or miss it entirely. The resulting burst size distribution decreases monotonically from zero (see Figure 2c).

Radial diffusion of the analyte places a lower limit on the sample stream diameter downstream of the point of sample introduction into the sheath flow. For example, rhodamine 6G, a fluorochrome weighing approximately 500 atomic mass units, has a diffusion constant of ~ 300 μm^2 s^{-1} in water and will, on average, diffuse ~ 1 μm from the sample stream centerline during the first millisecond following injection into an aqueous sheath flow and would likely miss the center of a femtoliter probe volume. To date, most investigations using femtoliter volumes have relied on diffusion to transport analyte molecules through the detection volume. The absolute detection efficiency (fraction of molecules in the analyzed sample that are actually detected) of such an arrangement is extremely low. For analyses where efficient detection of the analyte is required, it is best to choose the largest probe volume consistent with an acceptable signal-to-noise ratio for the application under study.

Time-correlated, single-photon counting (TCSPC) can be used to reduce background due to scattered laser light.[24] A mode-locked, picosecond laser pulse train is used to excite fluorescence. Arrival times of detected photons with respect to the excitation laser pulses are used to discriminate against Raman and Rayleigh scattered background light. Photons detected within ~ 1 ns of the excitation laser pulse are primarily due to scattered light; those detected outside of this time window are due to fluorescence. TCSPC allows the detection of single fluorochromes with good signal-to-noise ratios in probe volumes as large as a few picoliters. An additional benefit of TCSPC is the ability to measure τ_f for single molecules as they flow through the detection volume.[5,6,25]

Experimental Methods. Detailed descriptions of the SMD apparatus used for various applications in

(20) Kondilenko, I. I.; Korotkov, P. A.; Klimenko, V. A.; Demyanenko, O. P. *Opt. Spectrosc.* **1977**, *43*, 384−386.
(21) Mets, Ü.; Rigler, R. *J. Fluoresc.* **1994**, *4*, 259−264.
(22) Rigler, R.; Mets, Ü.; Widengren, J.; Kask, P. *Eur. Biophys. J.* **1993**, *22*, 169−175.
(23) Goodwin, P. M.; Ambrose, W. P.; Martin, J. C.; Keller, R. A. *Cytometry* **1995**, *21*, 133−144.
(24) Harris, T. D.; Lytle, F. E. Analytical Applications of Laser Absorption and Emission Spectroscopy. In *Ultrasensitive Laser Spectroscopy*; Kliger, D. S., Ed.; Academic Press: New York, 1983.
(25) Tellinghuisen, J.; Goodwin, P. M.; Ambrose, W. P.; Martin, J. C.; Keller, R. A. *Anal. Chem.* **1994**, *66*, 64−72.

our laboratory have been published elsewhere;[26−29] only a general description is given here. An excitation laser beam is focused to a circular spot with e^{-2} diameter between 10 and 50 μm at the center of the 250 × 250 μm^2 flow channel of a sheath flow cuvette. The smaller excitation beam diameters provide picoliter excitation volumes necessary for the detection of single fluorochromes; larger diameters are used when uniform illumination of the sample stream is needed for applications requiring well-resolved burst size distributions such as single fragment DNA sizing by LIF.[28] Samples are introduced into the sheath flow from a capillary located upstream of the focused excitation laser. Hydrodynamic focusing of the sample by the sheath flow produces sample streams with diameters in the range of 5−20 μm.[30] The sheath flow cell is mounted on a three-axis translation stage to allow precise alignment of the sample stream to the focused excitation laser. Fluorescence is collected at 90° to the flow and excitation laser axes using a 40×, 0.85 numerical aperture (NA) microscope objective. A slit located in the image plane of the collection objective with its long axis oriented parallel to the flow stream defines the detection volume. In order to have a well-defined detection volume, it is critical that the collection objective forms a good image of the excitation volume at the slit. A lower NA objective with good image quality is better than a high NA objective that collects more light but forms a poor image. The collection face of the sheath flow cuvette is fabricated to a coverslip thickness to accommodate the relatively short working distance (370 μm) of our collection objective. An optical collection efficiency of 9% was measured for this microscope objective and sheath flow cell combination.[23] Much higher efficiencies are obtainable using elliptical, parabolic, and spherical reflective optical collection arrangements, but these nonimaging systems cannot be used in combination with spatial filtering to give well-defined probe volumes.[31] Filters located behind the slit limit the spectral bandwidth of the light reaching the detector. Care is taken to use optical components that do not fluoresce when illuminated by scattered laser light. We use photomultiplier tubes (PMTs) and silicon avalanche photodiodes (SAPDs) as detectors. Photon counting SAPDs are a new class of detectors that have become commercially available recently. The main advantage of these detectors is their high photoelectric efficiency, typically better than 40 % in the mid-visible spectral region. A drawback is the relatively long dead time (~1 μs) which limits the maximum counting rates. Use of photon counting SAPDs for SMD is discussed in detail by Li and Davis.[32] With SAPD detection, the overall fluorescence photon detection efficiency of our apparatus (including the spectral band-pass filter transmission) is approximately 1%.

Table 1. Background Burst Rate Reduction by Laser Photolysis

	burst rate (s^{-1})	
	photolysis off	photolysis on
ultrapure water	7.7	1.2
exonuclease buffer: 5 mM $MgCl_2$ + 0.05 mM Tris−HCl + 150 units/mL exonuclease III	90	7.0

The photon counting and data acquisition electronics used in our laboratory are described elsewhere. We use continuous wave laser excitation and simple photon counting whenever possible, e.g., for DNA fragment sizing.[8,28,33] Mode-locked laser excitation and TCSPC are used for higher sensitivity applications requiring better discrimination against Raman and Rayleigh scattered background light.[26]

Fluorescence Background Reduction. To date, our experimental strategies have been geared toward detection of fluorochromes that absorb in the blue-green portion of the visible spectrum and emit in the yellow-orange region. Dyes were chosen for their favorable photophysical properties (large absorption cross-sections, high fluorescence quantum yields, good photostability) as well as the availability of good laser light sources for their excitation. Our experience has shown that most buffers useful for bioassays contain fluorescent impurities that give both large bursting and nonbursting backgrounds when examined under the conditions described above. Even with painstaking care in the selection of buffer components, background burst rates are consistently at least an order of magnitude higher than from ultrapure water. We have demonstrated an on-line laser photolysis arrangement to reduce fluorescent backgrounds from these buffers.[34] Briefly, the setup consists of a hollow fused silica capillary with an inner diameter of 500 μm and a length of about 80 cm secured at both ends and pulled taut. Sheath fluid is flowed through the capillary and into the SMD flow cell. Excitation laser light coupled into the input end of the capillary propagates coaxially with the sheath fluid. Fluorescent impurities that absorb at the excitation laser wavelength are repeatedly excited as the buffer flows through the capillary and are photolyzed before leaving the capillary. Some results obtained with this setup are summarized in Table 1, see ref 34 for more details. For comparison, a 10^{-13} M aqueous solution of tetramethylrhodamine isothiocyanate (TRITC), the analyte for which the detection system was optimized, gave a burst rate of 35 s^{-1}.

Efficient Detection of Single Molecules. Efficient detection of single fluorochrome tags is a prerequisite for our single fragment DNA sequencing method (see below). We have demonstrated detection efficiencies >90% for single TRITC fluorochromes delivered to a ~3 pL probe volume.[29] TRITC was chosen because TRITC-labeled nucleotides have been successfully incorporated into DNA sequences.[7]

Fluorescence was excited using a mode-locked dye laser operated at 554 nm, near the absorption maxima of TRITC and the labeled nucleotide (TRITC-dUTP).

(26) Goodwin, P. M.; Wilkerson, C. W., Jr.; Ambrose, W. P.; Keller, R. A. *Proc. SPIE* **1994**, 1895, 79−89.
(27) Johnson, M. E.; Goodwin, P. M.; Ambrose, W. P.; Martin, J. C.; Marrone, B. L.; Jett, J. H.; Keller, R. A. *Proc. SPIE* **1994**, 1895, 69−78.
(28) Goodwin, P. M.; Johnson, M. E.; Martin, J. C.; Ambrose, W. P.; Marrone, B. L.; Jett, J. H.; Keller, R. A. *Nucleic Acids Res.* **1993**, *21*, 803−806.
(29) Goodwin, P. M.; Affleck, R. L.; Ambrose, W. P.; Demas, J. N.; Jett, J. H.; Martin, J. C.; Reha-Krantz, L. J.; Semin, D. J.; Schecker, J. A.; Wu, M.; Keller, R. A. *Exp. Tech. Phys.* **1995**, *41*, 279−294.
(30) Zarrin, F.; Dovichi, N. J. *Anal. Chem.* **1985**, *57*, 2690−2692.
(31) Seitzinger, N. K.; Martin, J. C.; Keller, R. A. *Appl. Opt.* **1990**, *29*, 4255−4258.
(32) Li, L. Q.; Davis, L. M. *Rev. Sci. Instrum.* **1993**, *64*, 1524−1529.
(33) Petty, J. T.; Johnson, M. E.; Goodwin, P. M.; Martin, J. C.; Jett, J. H.; Keller, R. A. *Anal. Chem.* **1995**, *67*, 1755−1761.
(34) Affleck, R. L.; Ambrose, W. P.; Demas, J. N.; Goodwin, P. M.; Schecker, J. A.; Wu, M.; Keller, R. A. *Anal. Chem.* **1996**, *68*, 2270−2276.

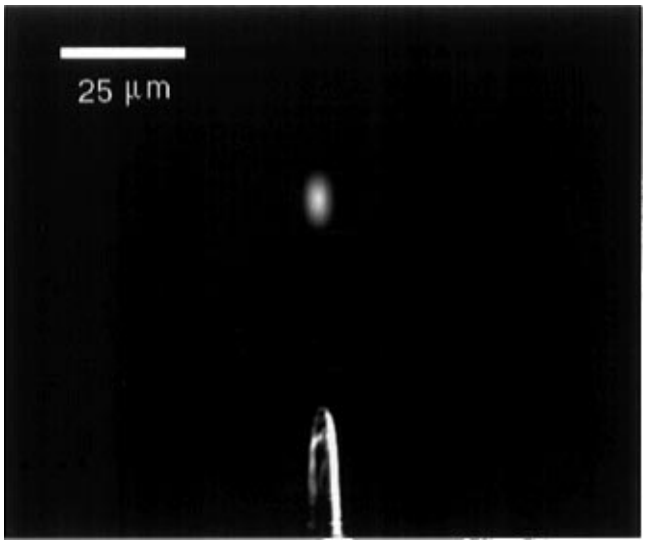

Figure 3. Electrokinetic delivery of TRITC from a drawn micropipet. View of the capillary tip and sample stream fluorescence seen through the 40× collection objective. The sheath flow direction is from bottom to top in the picture. The end of the capillary is located ~50 μm upstream of the excitation laser. Conditions: sheath volumetric flow rate, 20 μL/min; sample flow velocity, ~1 cm/s; micropipet tip inner diameter, <1 μm; electrokinetic drive voltage, +1500 V.

TCSPC was used to discriminate against scattered light. A 1×10^{-6} M solution of TRITC dissolved in a salt buffer was delivered electrokinetically into a sheath flow from a pulled capillary tip, <1 μm in diameter, located approximately 50 μm upstream of the focused excitation laser beam. Figure 3 shows the micropipet and fluorescence from the illuminated sample stream as viewed through the 40 × fluorescence collection objective. For this picture, the electrokinetic drive voltage across the capillary was set to +1500 V to deliver sample at a rate sufficient to make the sample stream fluorescence visible to the naked eye. The oblong shape of the fluorescence excited by the laser shows that the sample stream diameter is smaller than the circular waist of the focused excitation laser (e^{-2} diameter, 15 μm). Reduction of the electrokinetic drive voltage allowed sample delivery at extremely low rates. This is shown in Figure 4. Panels a−d show 200 ms time sequences of the number of gated photoelectrons (fluorescence photons detected in a time window excluding the laser pulse) detected in successive 0.25 ms intervals. The electrokinetic drive voltage was lowered from 2.25 to 1.5 V in steps of 0.25 V. At 2.25 V the delivery rate of TRITC molecules is too high for SMD; i.e., more than one molecule is in the probe volume at any given time. In panel d, the sample delivery rate was low enough that fluorescence bursts from individual TRITC molecules crossing the probe volume are visible. The similarity in the sizes of the photon bursts in panel d is a consequence of all TRITC molecules in the sample stream passing through the center of the detection volume and receiving approximately the same integrated excitation irradiance.

A size distribution of fluorescence bursts detected from TRITC molecules delivered under conditions similar to those in panel d of Figure 4 is shown in panel a of Figure 5. Approximately 64 s of data were searched for photon bursts using an algorithm described elsewhere.[26] The peak in the distribution at

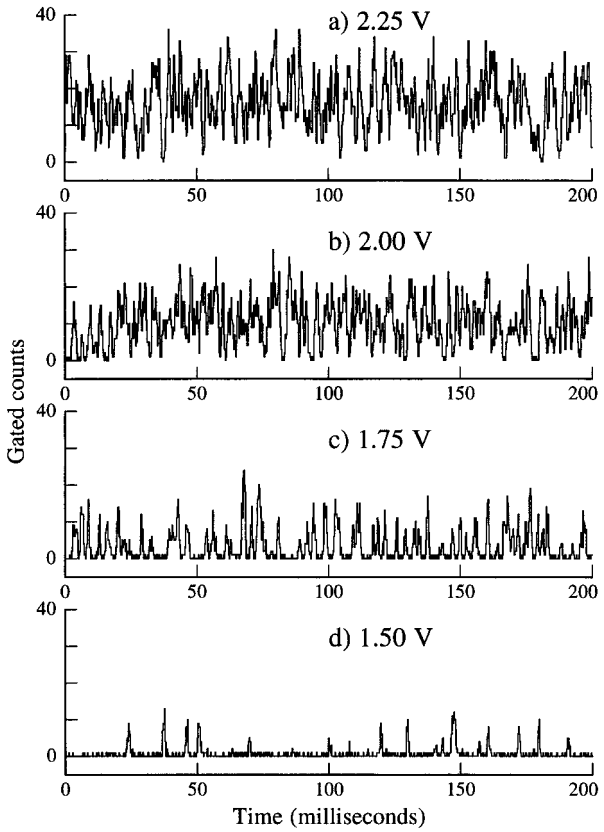

Figure 4. Detection of fluorescence from TRITC delivered electrokinetically from a drawn capillary. The geometry is similar to that shown in Figure 3. Fluorescence counts (gated counts) detected in 0.25 ms bins over 200 ms intervals are shown for four electrokinetic drive voltages: (a) 2.25 V, (b) 2.00 V, (c) 1.75 V, (d) 1.50 V. Photon bursts due to individual TRITC molecules are visible at the lowest drive voltage (d). For this experiment, the average excitation laser power was 10 mW, and the sheath volumetric flow rate was 25 μL/min.

~40 photoelectrons (PE) is due to bursts detected from single TRITC molecules crossing the probe volume. The shoulder on the high side of the main peak extending past 100 PE is due to bursts detected from two or more TRITC molecules passing through the probe volume simultaneously. The burst size distribution demonstrates clearly that we are able to deliver analyte molecules through the central portion of the ~3 pL detection volume and detect these molecules with high efficiency. When the sample stream diameter is larger than the detection volume, then the burst size distribution decreases monotonically from zero PE as shown in Figure 2c. For the blank, shown with filled circles in panel a of Figure 5, approximately 64 s of data from the sheath flow alone was searched for bursts. The monotonic decay of the blank burst size distribution reflects the larger diameter of the sheath flow compared to the size of the probe volume (see Figure 2c).

A Monte Carlo simulation was used to verify that the observed burst size distribution is due to TRITC molecules. The simulation accounts for spatial variations in the intensity of the focused excitation laser and the light gathering efficiency of the optical collection system as well as optical saturation, photobleaching, and diffusion of TRITC.[29] Analyte molecules were delivered to the probe volume at an average rate of 100 s^{-1}. The result of searching 64 s of synthetic data for bursts is shown in panel b of

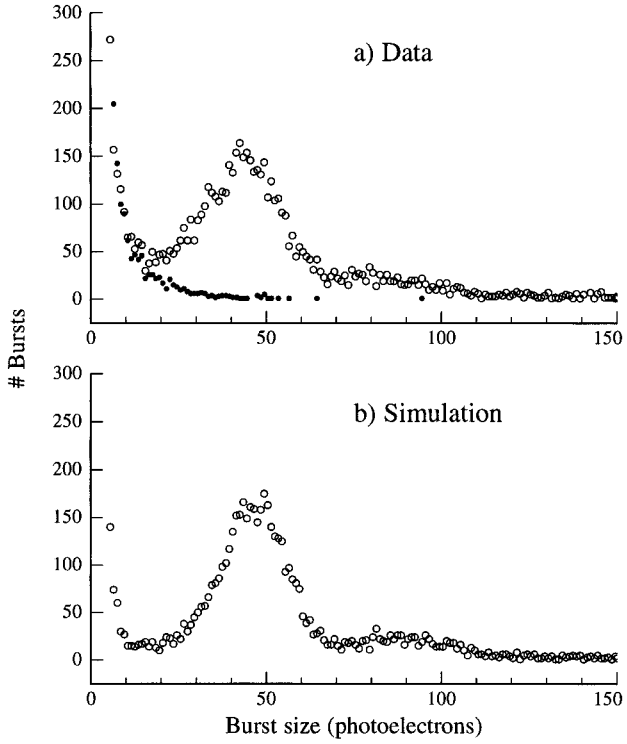

Figure 5. Experimental and synthetic photon burst size distributions: (a) open circles, measured burst size distribution for TRITC delivered electrokinetically from a drawn capillary; filled circles, measured background (sheath) burst size distribution; (b) photon burst size distribution obtained from Monte Carlo simulation data. Each distribution was compiled from 64 s of data. For this experiment, the average excitation laser power was 20 mW, and the sheath volumetric flow rate was 20 μL/min.

Figure 5. The good agreement between the experiment and the simulation corroborates our assertion that we are detecting single TRITC molecules. For a detection threshold set at 20 PE, the simulation predicts that >90% of the TRITC molecules leaving the capillary are detected. According to the simulation, approximately 10% of the molecules photobleach while crossing the probe volume; about half of these are detected before they photobleach.

Applications

Single-Molecule DNA Sequencing. We are developing a flow-based method to sequence single fragments of DNA.[7,29,35] Our technique involves (1) polymerase incorporation of fluorescently tagged nucleotides into a target sequence, (2) anchoring the labeled DNA strand in a flowing stream, (3) sequential exonuclease release of the tagged nucleotides from the free end of the DNA fragment, and (4) efficient detection and identification of the cleaved, tagged nucleotides to give the DNA sequence. The method has the potential for reading long ($\sim 10^4$ bases), contiguous DNA sequences in contrast to current, gel-based sequencing technologies that have read lengths of less than 1000 bases.

We have demonstrated the detection of single, TRITC-labeled nucleotides enzymatically cleaved from as few as 15−30 DNA fragments, attached to a 2.8 μm diameter microsphere held in a sheath flow.[29,35] A buffer containing an exonuclease is flowed past TRITC-labeled DNA fragments held upstream of a ~3 pL detection volume. As the exonuclease digests the DNA fragments, individual TRITC-labeled nucleotides are swept through the probe volume and detected. On-line laser photolysis was used to reduce the background to manageable levels (see Table 1) without significant reduction of the activity of the exonuclease.[34] The turnover rate of *Escherichia coli* exonuclease III on fluorescently labeled DNA in flow was measured to be ~7 nucleotides per DNA fragment per second at 36 °C. This is approximately the same as the rate measured for this enzyme on native DNA under static, saturated (excess enzyme) conditions. Work is underway to find enzymes with significantly higher turnover rates on fluorescently labeled DNA. At our current background burst rate of $\sim 10\ s^{-1}$, an enzyme turnover rate of at least 50 nucleotides per DNA fragment per second is necessary to detect cleaved, fluorescently tagged nucleotides from a single DNA fragment above background.

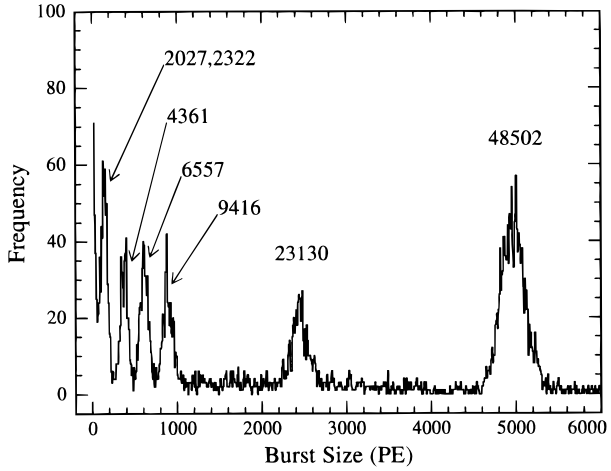

Figure 6. Size distribution of photon bursts detected from individual TOTO-1 stained DNA fragments. A dilute ($\sim 10^{-13}$ M) mixture of λ DNA (48 502 bp) and a *Hin*dIII digest of λ DNA (125, 564, 2027, 2322, 4361, 6557, 9416, and 23 130 bp) stained with TOTO-1 was passed through the probe volume of an ultrasensitive flow cytometer. Fragment lengths, in base pairs, are indicated above the peaks. The 2027 and 2322 bp fragments were not resolved from each other; the two smallest fragments (125 and 564 bp) were not detectable above the background in this experiment. A linear correlation coefficient of 0.9997 was found between the distribution peak positions and the known fragment lengths. See the paper by Petty et al.[33] for more details.

Single-Molecule DNA Fragment Sizing. Recently, we[8,28,33] and others[36] have developed a flow cytometry-based method to determine the length (number of base pairs (bp)) of individual DNA fragments. Briefly, DNA fragments are stained stoichiometrically, with respect to their lengths, with an intercalating dye. A dilute solution of these stained fragments, hydrodynamically focused to a sample stream <20 μm in diameter, is flowed through a ~30 pL detection volume. A size distribution of fluorescence bursts detected from individual DNA fragments is compiled. The burst size distribution is linearly related to the fragments' length distribution. An example of such a burst size distribution is shown in Figure 6. A sample with a known distribution of DNA

(35) Schecker, J. A.; Goodwin, P. M.; Affleck, R. L.; Wu, M.; Martin, J. C.; Jett, J. H.; Keller, R. A.; Harding, J. D. *SPIE* **1995**, *2386*, 4−12.

(36) Castro, A.; Fairfield, F. R.; Shera, E. B. *Anal. Chem.* **1993**, *65*, 849−852.

fragment lengths was stained with the intercalating dye thiazole orange homodimer (TOTO-1). Fluorescence bursts detected from approximately 5000 of these stained fragments (~0.1 pg of DNA), during a run lasting several minutes, were analyzed to produce the burst size distribution shown in the figure. Advantages of this method over traditional gel electrophoresis techniques are (1) high sensitivity, the analysis requires less DNA, picograms versus nanograms, (2) shorter analysis time, minutes versus hours, (3) superior resolution of large fragments, fluorescence burst sizes are linearly proportional to the fragment lengths whereas electrophoretic motion is inversely proportional to the logarithm of the fragment lengths, and (4) insensitivity to DNA conformation, the method works well with supercoiled DNA fragments.[8] We have used this method to size DNA fragments between 500 and 167 000 bp in length. To size larger fragments, extreme care will have to be taken not to shear (break up) the sample prior to analysis. Size resolution of small fragments will ultimately be limited by the width of the number distribution of dye molecules that intercalate a uniform length population of DNA fragments. Since the DNA is intercalated at a density of approximately 5 bp/dye, this method will not achieve the single base pair resolution that electrophoresis methods are capable of for small (<1000 bp) DNA fragments.

Conclusions

SMD in liquids, which began as an experimentalist's challenge, has become a powerful research tool. Ultrasensitive fluorescence detection will have an increasing impact on fields where fluorescence detection and quantification are broadly applied, e.g., analytical chemistry, biology, and medicine. Recent efforts toward the ultraminiaturization of analytical instrumentation for increased speed and decreased sample sizes will benefit from the extreme detection sensitivity from picoliter and smaller detection volumes provided by SMD techniques. The ability to monitor fluorescence from a single molecule in solution allows the direct observation of processes at the single molecule level and the measurement of molecular properties that are averaged out in bulk measurements on large ensembles. SMD is a new way of doing analytical chemistry, and new applications will arise.

Our approach to sensitive fluorescence detection in flow has benefited greatly from interactions with the National Flow Cytometry Resource at Los Alamos National Laboratory. We thank H. L. Nutter for his expert technical assistance in the laboratory. The research described here was supported by the Los Alamos Center for Human Genome Studies under U. S. Department of Energy Contract W-7405-ENG-36, the Los Alamos National Flow Cytometry Resource under NIH Grant RR01315, and Los Alamos National Laboratory internal funds.

AR950250Y